ACS OMEGA

Open Access

http://pubs.acs.org/journal/acsodf

Article

Selective Naked-Eye Detection of Lung Squamous Cell Carcinoma Mediated by lncRNA SOX2OT Targeted Nanoplasmonic Probe

Nastaran Roknabadi, Yasaman-Sadat Borghei,* Seyedeh Saina Seifezadeh, Bahram M. Soltani, and Seyed Javad Mowla*

Cite This: *ACS Omega* 2024, 9, 37205−37212

Read Online

ACCESS | Metrics & More | Article Recommendations

ABSTRACT: The application of nanobiotechnology in biomolecule detection can provide fast and accurate tests for diagnosing molecular changing-associated diseases. The use of AuNPs-thiolated probe conjugates has long been considered as an alternative method for the detection of specific DNA/RNA targets. Here, we present a colorimetric direct detection method for the SOX2OT transcript, long noncoding RNAs (lncRNAs), by using a poly guanine tail (G12) as a template for in situ synthesis of gold nanoparticles (AuNPs) without any chemical modification or DNA labeling. We have then developed this proposed detection system based on two complementary sequences of long noncoding RNA SOX2OT with an extra strand of poly G12. Using this method, we were able to differentiate lung squamous cell carcinoma from adenocarcinoma samples. Based on this disclosure, this invention provides a simple visual method to detect specific lncRNA sequences without the need for amplifying the target lncRNA and discriminate squamous cell carcinoma from adenocarcinoma samples. Our invention provides a diagnostic kit to detect RNA by means of direct detection (PCR-free) of the lncRNA by in situ synthesis of AuNPs based on two probes with an extra strand of poly G12.

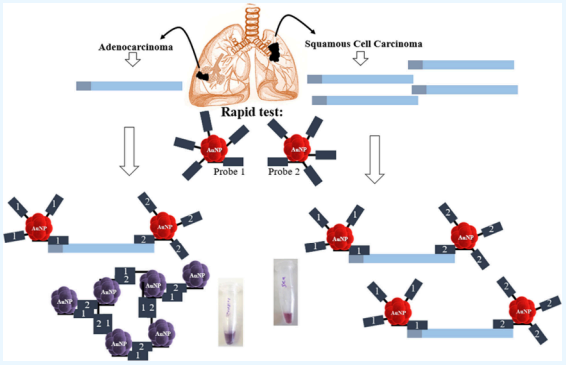

1. INTRODUCTION

Lung cancer is among the most frequently diagnosed cancers and the leading cause of cancer-related mortality worldwide.[1] Lung cancer is a very heterogeneous disease that, in terms of histology, is classified into two main groups: nonsmall cell lung cancer (NSCLC) and small cell lung cancer (SCLC). Adenocarcinoma (ADC), squamous cell carcinoma (SCC), and large-cell lung carcinoma (LCLC) are three types of NSCLC.[2]

Optimal treatment for lung cancer patients depends on an accurate diagnosis. At the moment, the most commonly used lung cancer diagnostic tools include chest radiography, computed tomography (CT), bronchoscopy, biopsy, and sputum cytology.[3] To differentiate SCC from ADC, biopsy cytology and immunohistochemistry (IHC) staining are the most widely utilized approaches.[4] Using these methods, only 15% of lung cancers are detected in their early stages.[5] Current diagnostic tools for lung cancer have a number of shortcomings, including poor accuracy, low sensitivity, high costs, and invasive procedures.[6] It is therefore urgent to identify sensitive and specific tools for the early detection of lung cancer.[7]

The identification of lung cancer biomarkers has been made possible by recent developments in molecular techniques and analytical frameworks.[8] As our understanding of the molecular mechanisms and biological roles of lncRNAs in lung cancer has increased, scientists have turned their attention to using these molecules as biomarkers for lung cancer diagnosis and prognosis.

SRY-box transcription factor 2 (SOX2) overlapping transcript (SOX2OT) is a lncRNA located on the chromosome 3q26.3 locus.[9] In recent years, SOX2OT has been extensively investigated for its role in tumorigenesis. Studies have shown that SOX2OT is a key regulator of cancer stem cells and plays an important part in tumor progression, proliferation, invasion, migration, and growth of cancer cells, as well as suppressing their apoptosis.[10]

There are several current methods for evaluating nucleic acid biomarkers, including next generation sequencing (NGS), real-time PCR and microarray-based comparative genomic hybridization (array CGH); despite their remarkable benefits, these methods are costly, time-consuming, complex, and occasionally nonspecific.[11,12] In this regard, the emergence of practical

Received: May 14, 2024
Revised: July 25, 2024
Accepted: August 9, 2024
Published: August 21, 2024

https://doi.org/10.1021/acsomega.4c04565
ACS Omega 2024, 9, 37205−37212

Scheme 1. View of the Proposed Method in the Detection of ADC and SCC Lung Tumor Samples

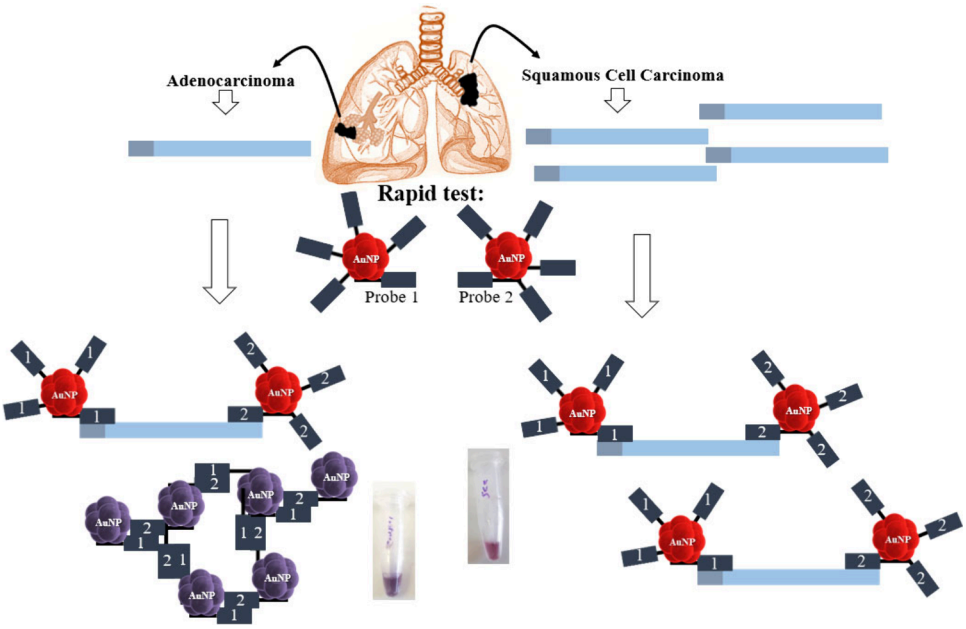

applications of cancer biomarkers is largely attributed to the development of user-friendly methods for molecular analysis.

Recent advances in the field of nanotechnology have contributed to the development of novel methods for the detection of various biomarkers.[13−16] Over the past few years, colorimetric assays based on plasmonic nanoparticles have been developed. Due to their localized surface plasmon resonance (LSPR) properties, these NPs serve as an effective tool for detecting a variety of compounds. For instance, researchers used DNA-coated AuNPs to determine the presence of mRNA in live *Hydra vulgaris* animals. Surprisingly, the AuNPs were not poisonous to this animal and did not cause death.[17]

This study reports a visual method for differentiation between SCC and ADC by using an extra strand of poly G with a "sticky end" that is complementary to the lncRNA SOX2OT target sequence. Here, the extra strand of poly G is being used as a template for in situ formation of AuNPs without any chemical functionalities. Therefore, in the presence of lncRNA, two probes are designed in such a way that after hybridization they are far from each other. We have a localized surface plasmon resonance (LSPR) band at 530 nm. However, in the absence of lncRNA, the two probes are dimerized, and a red shift in their LSPR is observed. So, as shown in Scheme 1, this method enables the differentiation of SCC patients with high expression level of lncRNA SOX2OT from ADC patients with a naked-eye (equipment-free), label-free (cost-effective) and PCR-free (to speed up) method.

2. EXPERIMENTAL SECTION

2.1. Materials and Methods. Chloroauric acid ($HAuCl_4$-$4H_2O$), NaH_2PO_4 and HEPES (4-(2-hydroxyethyl)-1-piperazineethanesulfonic acid) were purchased from Sigma-Aldrich. All chemicals were of analytical grade or of the highest purity available. Deionized water with a resistivity of >18 MΩ cm was acquired from a Millipore Milli-Q system. The following oligonucleotides were synthesized by Pishgam Biotech (Tehran, Iran): Oligonucleotide samples were purified by PAGE and prepared with TE buffer (1 M Tris-HCl and 0.5 M EDTA).

- Probe 1 (P1): GGGGGGGGGGGGTTGGATC-TCAGAGTTGATTGTTTTC
- Probe 2 (P2): AGACGATAGAAGTCTTAGAAT-GATGCGGGGGGGGGGG
- Primer (F): CAGCTGATAACAAGCAAAAG
- Primer (R): CTGGCAAAGCATGAGGAACTATC

2.2. Cell Culture. Calu-6 (Human lung cancer cell line), KYSE-30 (human esophageal cancer), and HEK293T were obtained from The National Cell Bank of Iran. KYSE-30 and HEK293T were cultured in DMEM (gibco, USA) supplemented with 10% fetal bovine serum (FBS) (gibco, USA) and 1% penicillin-streptomycin (gibco, USA). Calu-6 cells were cultured in RPMI (gibco, USA) supplemented with 10% fetal bovine serum (FBS) (gibco, USA) and 1% penicillin-streptomycin (gibco, USA). Cells were incubated in 37 °C in a water-saturated atmosphere with 5% CO_2.

2.3. Tissue Samples. Lung tissues were selected from the Iran National Tumor Bank, founded by the Cancer Institute of the Tehran University of Medical Sciences. The clinicopathological information on each patient was obtained as well. Immediately after being collected from patients, the samples were frozen in liquid nitrogen and then stored at −80 °C until they were selected for RNA extraction. The biopsies were obtained from patients before they consumed any special medication or underwent chemotherapy. This study was approved by the Ethics Committee of Tarbiat Modares University (Number: IR.MODARES.REC.1400.082).

2.4. RNA Extraction and cDNA Synthesis. Total RNA was extracted from homogenized tissues and cell lines using a One Step-RNA reagent (BIO BASIC, Canada) according to the manufacturer's instructions. The quality and quantity of the extracted RNA were assessed with the NanoDrop ND-1000 Spectrophotometer (ThermoFisher, USA) and the integrity and quality of the RNA were also evaluated by gel electrophoresis. In order to eliminate any possible DNA contamination, DNase treatment was performed using a DNase I RNase-free kit (ThermoFisher, USA). The reaction was conducted at 37 °C for 30 min. In order to inactivate the DNase enzyme, a 10 min incubation with EDTA at 65 °C was performed. 1 μg of total

https://doi.org/10.1021/acsomega.4c04565
ACS Omega 2024, 9, 37205−37212

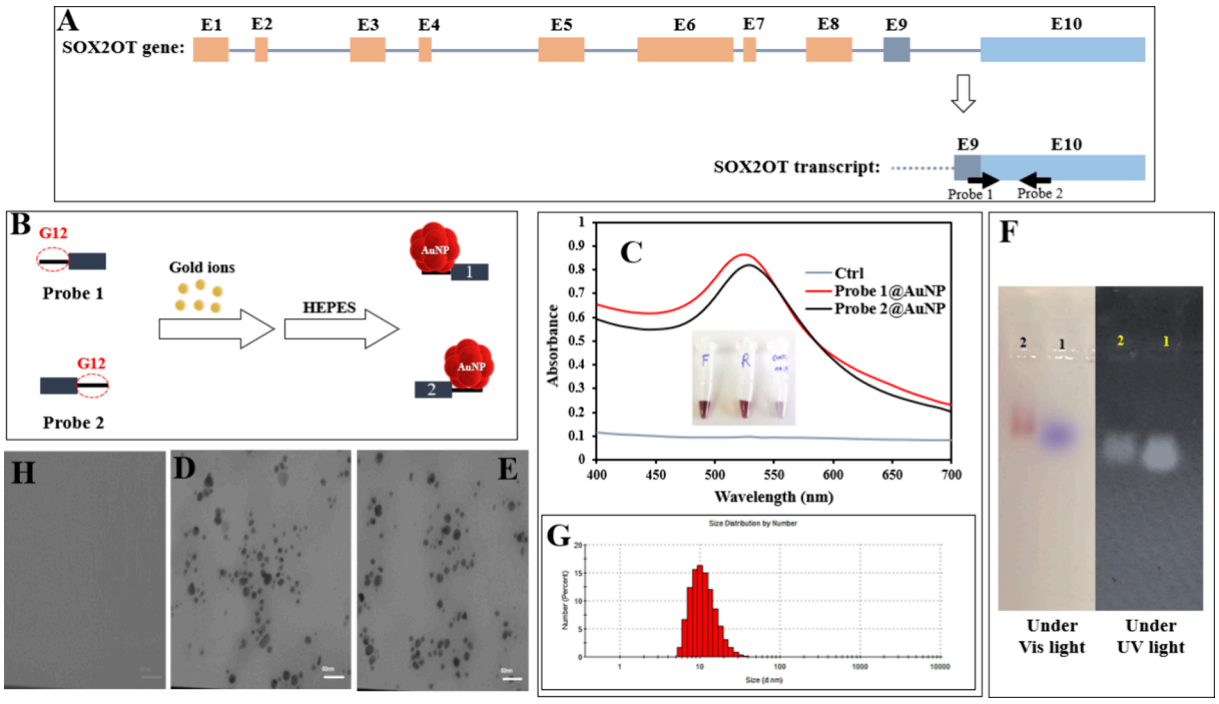

Figure 1. (A) Schematic presentation of the SOX2OT gene and its transcripts. The designed probes (P1, P2) and lncRNA target sites are indicated by arrows. (B) Schematics of AuNP formation using an extra strand of poly G12 of two probes. (C) Their absorption spectra and their photos under visible light. TEM images of the synthesized AuNPs using P1 (D), P2 (E), and without any oligonucleotide (H). (F) Agarose gel electerophoresis image of (lane 1) the DNA probe alone as a control and (lane 2) DNA probe@AuNPs. The first line from left to right is DNA (probe)@AuNPs and the second line is the DNA (probe) alone sample. (G) DLS analysis on the basis of the number distribution of synthesized DNA(probe)-AuNPs.

RNA was used to synthesize the first strand of cDNA by the RevertAid First Strand cDNA Synthesis Kit (ThermoFisher, USA). The procedure was carried out according to the instructions provided by the manufacturer.

2.5. Quantitative Real-Time Polymerase Chain Reaction (qRT-PCR). qPCR was performed using a 5× HOT FIREPol EvaGreen qPCR Mix Plus (Solis BioDyne, Estonia) in an Applied Biosystems StepOnePlus Real-Time PCR instrument (Applied Biosystems, USA). A PCR reaction mixture containing 1.5 μL of cDNA, 2 μL of EvaGreen, 0.5 μL of each primer (5 μM), and a sufficient amount of dH_2O were prepared, and the thermal cycling was performed under the following conditions: initiation at 95 °C for 10 min, a total 45 cycles of denaturation at 95 °C for 15 s, annealing at 57 °C for 20 s, and extension at 72 °C for 20 s were followed by a melt curve stage. All reactions were conducted in duplicates. In order to confirm the accuracy of the PCR amplification, melt curve analysis was performed, and PCR products were run on a 2% agarose gel and sequenced as well. The relative expression of SOX2OT was measured using the $2^{-\Delta\Delta CT}$ method, and GAPDH mRNA was used as the reference internal control of this experiment.

2.6. Agarose Gel Electrophoresis Analysis. Agarose gel (2% v/v) was prepared with 1× TBE buffer. 5 μL of samples were prepared with loading dye and loaded into a gel. The electrophoresis was run at 50 mV and for 20 min and visualized by a UV transilluminator (312 nm).

2.7. PolyG-Mediated Synthesis of DNA−AuNPs. DNA-AuNPs probes were prepared by mixing 5 μL of oligonucleotide (100 μM) with 50 μL of HEPES (5 mM) and adding 1 μL of $HAuCl_4$ (50 mM) to this mixture.[18] The mixture was vortexed briefly, and the solution changed after a few seconds from gray to red. The mixtures were incubated at room temperature for 30 min to complete the synthesis process. This procedure was performed separately for each probe (P1 and P2).

2.8. DNA Hybridization. After the finalization of the synthesis of Au-NPs on oligonucleotide probes, 25 μL of probe 1 was mixed with 25 μL of probe 2. The mixture was vortexed, and 25 μL of it was added to the reaction solution containing 2000 ng of total RNA. After a 5 min incubation at room temperature, 2 μL of NaCl solution (2 mM) was added to them. This mixture was then denatured at 90 °C for 5 min. Then, during the annealing process, the temperature is slowly decreased to room temperature to form DNA hybridizations.

2.9. Bioinformatics Analysis and Plotting ROC Curve. The in-silico analysis of SOX2OT expression in lung tumors was performed using the online tool FireBrowse (http://firebrowse.org/). This web site provides a differential gene expression analysis on TCGA data. The statistical analysis was conducted using GraphPad Prism 8.4.0 software. Unpaired *t* test was used in order to determine the significance of the differences between two groups. One-way ANOVA was chosen as the statistical test to compare more than two groups. Statistical significance was defined as a *P*-value of <0.05. In order to assess the sensitivity and specificity of SOX2OT for discriminating between SCC and ADC samples, a receiver operating characteristic (ROC) curve analysis was performed.

3. RESULTS AND DISCUSSION

3.1. Probe Design and Characterization of Synthesized DNA-AuNPs. The main challenge in this method is designing two DNA probes with a high specificity for the SOX2OT lncRNA sequence. To this aim, SOX2OT RNA sequence was obtained from NCBI, and the junction site was chosen to avoid possible hybridization with nonspecific DNA targets. As shown in Figure 1A, the forward probe was designed

https://doi.org/10.1021/acsomega.4c04565
ACS Omega 2024, 9, 37205−37212

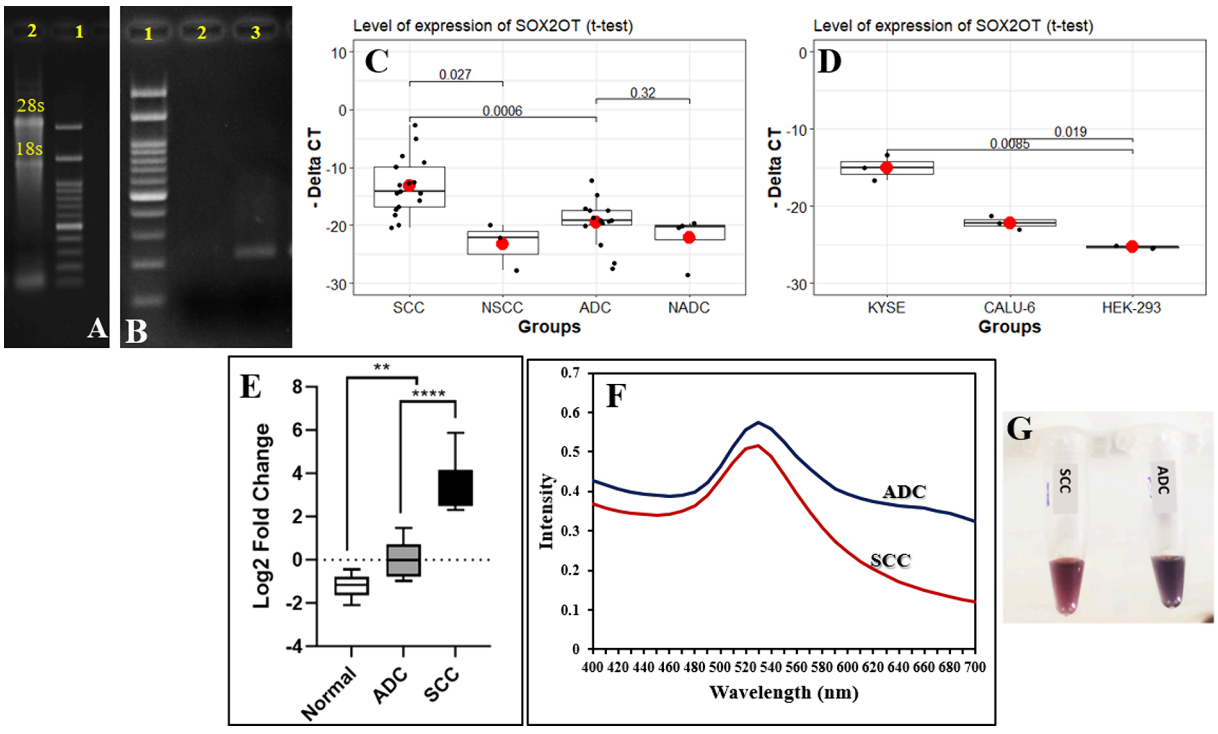

Figure 2. (A) Intact total RNA run on a gel will have sharp 28S and 18S rRNA bands. (B) PCR products for ADC and SCC samples run on agarose gel electrophoresis. (C) qRT-PCR analysis the expression levels of SOX2OT in four different SCC, non-SCC, ADC and Non-ADC samples and (D) in three cell lines. (E) Quantitative analysis of SOX2OT in two SCC and ADC samples. (F) UV−vis spectra of PCR product of both SCC and ADC samples. (G) The inset photograph displays them under visible light.

in the junction region of exons 9 and 10, and the reverse probe was designed on exon 10. In order to synthesize AuNPs on two designed probes, a ploy G_{12} sequence was added to the 5′ end of each probe as a DNA capping. In this process, two probes (P1 and P2) were mixed in $HAuCl_4$ and HEPES at three different reactions (one in the absence of any sequence, as a control; Figure 1B). After a few seconds, the color of the samples changed from colorless to red (except the control sample), and they were imaged under visible light as shown in Figure 1C (inset). In addition, their LSPR band was characterized by UV−vis spectroscopy (400 nm-700 nm). The absorption spectra of two DNA probes, P1 and P2, were recorded at around 530 nm, which are characteristics of the formed AuNPs (Figure 1C). As shown in the TEM analysis (Figure 1D, E), spherical and anisotropic AuNPs structures synthesized by P1 and P2 can be easily seen. It appears that poly G sequences at the 5′ end of each probe act as a scaffold for the synthesis of AuNPs. In addition, as shown in Figure 1G, DLS results give the size distribution of synthesized gold nanoparticles on the DNA scaffold.

As shown in Figure 1F, the agarose gel can be used to confirm the attachment of the aptamer to the AuNPs. For this purpose, in one lane, the aptamer was loaded after the synthesis of AuNPs, and in the other lane, the aptamer was loaded at the same concentration before the synthesis of AuNPs (aptamer alone). As you can see in the figure, the ruby color of AuNP can be seen with the naked eye and under visible light, but under UV light, two lanes can be compared both in terms of brightness and retardation. The brightness difference between the two lines indicates the concentration of aptamer involved in the AuNPs formation, so the brightness has decreased after synthesis. On the other hand, since the aptamer@AuNP complex is bigger than a naked aptamer, so the bands move at a different speed in the gel.

3.2. Differential Expression Levels of lncRNA SOX2OT in AC and SCC Samples. To investigate SOX2OT as a potential biomarker to classify AC from SCC, first, the quality of RNA total extracting was checked. The total RNA was run on a gel, and two intensive bands (28S and 18S rRNA bands) were observed against a light smear. As you see in Figure 2A, when the brightness of 28S band is twice that of 18S rRNA, it means that the extraction has been done completely and correctly. After that, a qRT-PCR method was used to study the expression profiles of the lncRNAs SOX2OT in ADC and SCC lung tumor samples and different cell lines (Calu-6, KYSE-30, and HEK293T). For this purpose, designed primers were employed to amplify fragments with a 217 bp length. The PCR products for ADC and SCC samples were run on agarose gel electrophoresis and as shown in Figure 2B, the line for the ADC sample has a very low expression of RNA, and the SCC sample, has higher levels of the target lncRNA SOX2OT with the sharp band. In addition, the results revealed that there is a significant difference (P = 0.0006) between ADC and SCC tumor samples and between KYSE-30 and HEK293T (P = 0.0085) in the SOX2OT expression level, and its expression level was significantly higher in the SCC samples than in the adenoma samples (Figure 2C) and also in KYSE cell lines than in the HEK293T (Figure 2D).

In order to verify the specificity of this method, we used the SOX2OT PCR product of SCC and ADC samples, and their SOX2OT expression levels were verified using both gel electrophoresis (Figure 2B) and qPCR (Figure 2E). For this purpose, after addition of P1 and P2 @AuNPs to each of the SCC and ADC PCR product solutions, the sample containing SOX2OT fragments (SCC) turned red, while the ADC sample turned purple (Figure 2F,G). These results indicated that proposed method works specifically.

https://doi.org/10.1021/acsomega.4c04565
ACS Omega 2024, 9, 37205−37212

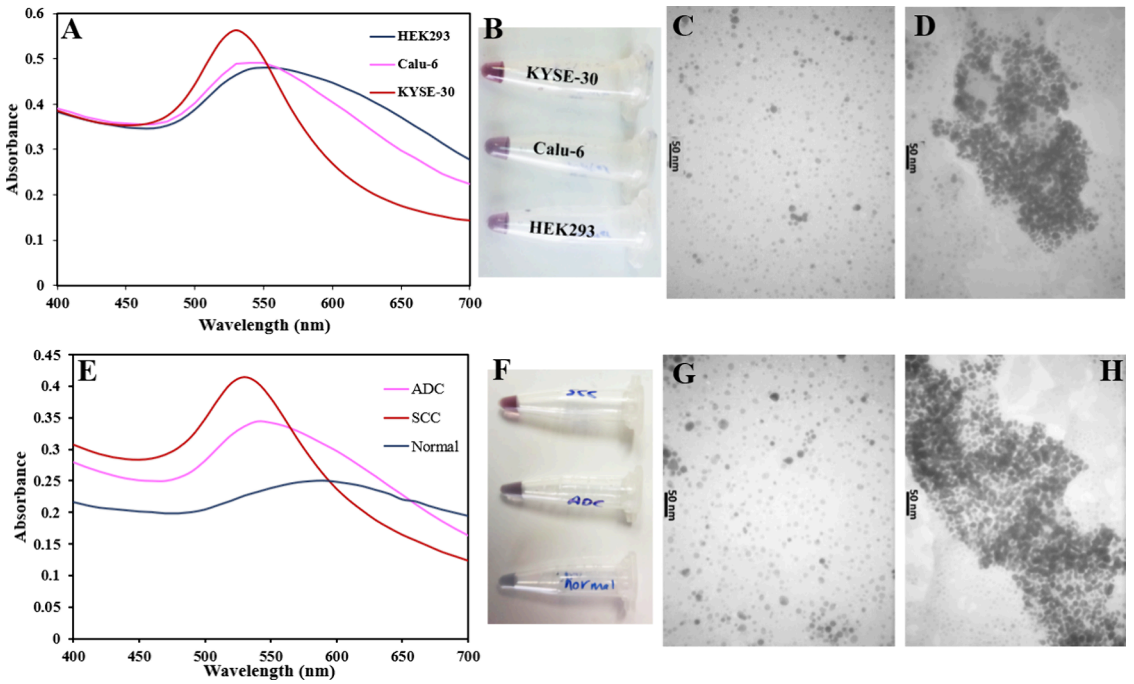

Figure 3. (A) UV−vis spectra of cell lines (KYSE-30, Calu-6, and HEK293). (B) The inset photograph displays them under visible light. TEM images of the reaction mixture with RNA extraction from (C) KYSE-30 and (D) Calu-6 cells. (E) UV−vis spectra of ADC and SCC samples. (F) The inset photograph displays them under visible light. TEM images of the reaction mixture with RNA extraction from (G) SCC and (H) ADC samples.

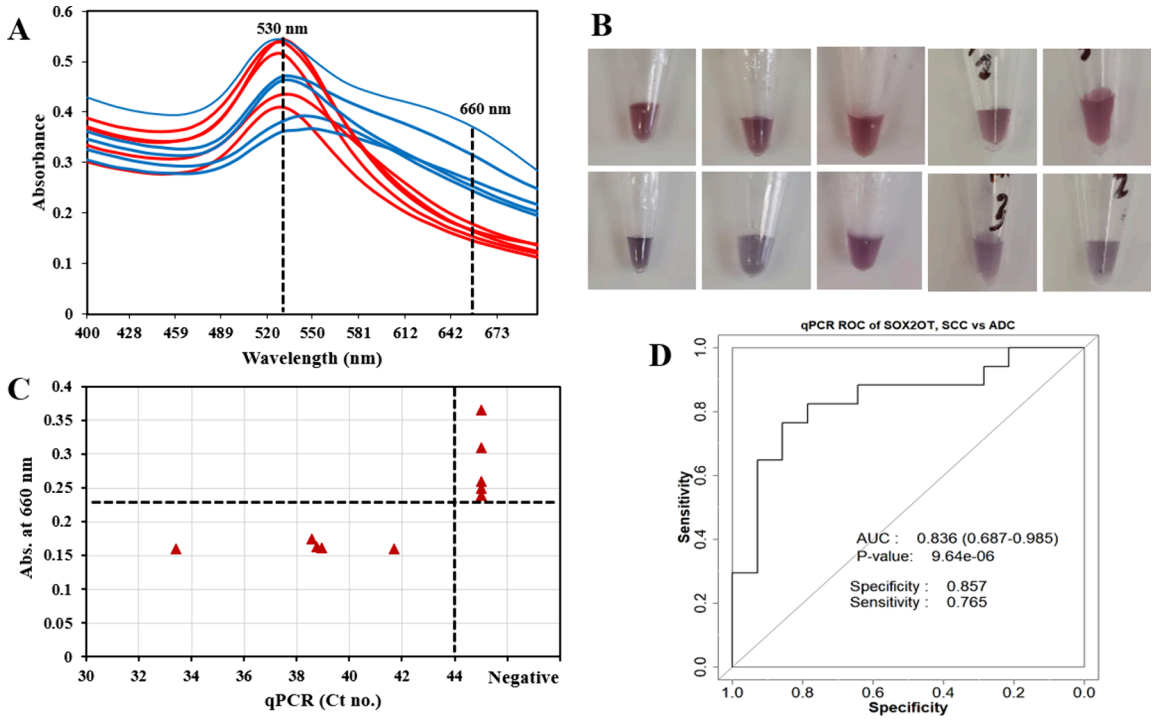

Figure 4. (A) UV−vis spectra of 5 AC and 5 SCC samples. (B) The inset photograph displays them under visible light. (C) Absorbance of the reaction mixture for 10 lung tumor tissue samples (5 AC and 5 SCC samples) at 660 nm. The patient samples were initially tested using a gold standard qRT-PCR kit, and the results were plotted against our proposed signals. The horizontal threshold line indicates the minimum absorbance at 660 nm to indicate that the samples are ADC by the proposed method. The vertical threshold line indicates that the maximum C_t number is about 44 to indicate that the sample is an SCC. (D) The ROC curve analysis for SOX2O*T* expression levels discriminating between SCC and AC patients determined a good degree of specificity and sensitivity.

3.3. Analytical Performance. In this work, we investigated the possibility of lncRNA detection using unmodified AuNPs as a colorimetric reporter. Assuming that after hybridizing the probes (P1 and P2) with lncRNAs, two probes remain stable at a distance that is larger than the radius of the nanoparticle ($d > r$), while in the absence of a target and also due to being polyvalent, they tend to hybridize with each other more. The characteristic

https://doi.org/10.1021/acsomega.4c04565
ACS Omega 2024, 9, 37205−37212

Table 1. Recently Methods for Detection of Long Noncoding RNAs

Labeled/Label-free	Probe	Biosensor type	Tumor/cell type	Sensing platform	LOD	ref
Label-free	RNA aptamer-Corn and magnetic based capture probe	Fluorescent biosensor	MCF-7 cells	Based on coupling duplex-specific nuclease (DSN)-assisted target recycling amplification with transcription-driven synthesis of fluorogenic RNA aptamer-Corns.	31.98 aM	22
Labeled	Biotin-probe-Cy3/Cy5 and magnetic based capture probe	Fluorescent biosensor	Lung tissues	Based on activating the ligation-transcription circuits to produce abundant functional RNAs. The resultant functional RNAs subsequently trigger DSN-assisted cyclic digestion of signal probes.	0.043 aM for lncRNA HOTAIR and 0.126 aM for lncRNA MALAT1	23
Labeled	three-way junction (3WJ) probes	Fluorescent biosensor	Breast tissues	Based on multiple cyclic enzymatic repairing amplification under an isothermal condition (50 °C).	0.87 aM	24
Label-free	ssDNA probe	Fluorescent biosensor	Breast cancer tissues	Based on recombinase polymerase amplification (RPA) without the involvement of thermal cycling and reverse transcription.	1.23 aM	25
Labeled	Magnetic bead−capture probe−multiple Cy5/Cy3-modified	Fluorescent biosensor	Cancer cells	Based on the target-catalyzed strand displacement reactions lead to the release of Cy5 and Cy3.		26
Labeled	Biotinylated uracil-labeled streptavidin gold nanoparticles	Fluorescent biosensor	Circulating lncRNAs	Based on fluorescence resonance energy transfer (FRET) system between AlexaFluor488 and PI.	up to 5 nM	27
Labeled	Thiolated probe	Electrochemical biosensor	Hepatocellular carcinoma	Based on Pt−Pd bimetallic nanodendrites/nanoflower-like clusters on graphene oxide/Au/horseradish peroxidase	0.247 fM/mL	28
Label-free	Thiolated/beta-actin and G-quadruplex probes	Electrochemical biosensor	The body's anti-HIV virus immunity	Based on Au/Rh-HNP@SWCNT complex and a reaction platform of an L-Cys film−Au nanoparticle.	0.8863 fM/mL	29
Labeled	Biotinylated dUTPs	Electrochemical/Colorimetric biosensor	Ovarian cancer	Based on an innovative merger of isothermal RT-RPA and HRP-catalyzed and magnetically purified.		30
Labeled	Amidated multiwalled carbon nanotube	Electrochemical biosensor	Lung cancer	Based on a gold nanocage coupled with an amidated multiwalled carbon nanotube	42.8 fM	31
Labeled	By the phosphate group	Photoelectrochemical biosensor	Cancer cell	Based on ZrO2@CuO bimetallic oxides and T7 Exoassisted signal amplification	0.12 fM	32
Labeled	FAM-RNA-Biotin	Lateral-flow-based	Tissue biopsies from prostate cancer patients	CRISPR−Cas-based reaction with a nanozyme-linked immunosorbent		33
Label-free	Guanine base capped anisotropic AuNPs	Colorimetric biosensor	Tissue biopsies from lung cancer	Based on direct-one-step clicking DNA to AuNPs and hybridization mediated assay		Here

https://doi.org/10.1021/acsomega.4c04565
ACS Omega 2024, 9, 37205−37212

LSPR peak of AuNPs at 530 nm shifts to a longer wavelength in the absence of lncRNAs, with a color change from red to purple.

This hypothesis was tested with cell lines and two types of human lung cancer samples: the adenoma sample, which according to previous reports[19−21] and our qRT-PCR results has a very low expression of RNA, and the SCC sample, which has higher levels of the target lncRNA SOX2OT. By adding two specific DNA probes (P1@AuNPs and P2@AuNPs) and forming a heteroduplex with the lncRNA SOX2OT in the SCC and KYSE samples, the LSPR bands were recorded at 530 nm (Figure 3). In samples containing lower levels of lncRNA (ADC and HEK293T), the absorption peak shifts to longer wavelengths, and the color changes to purple.

In addition, the aggregation of AuNPs was determined through TEM images, which show that two DNA probes are at longer distances in the presence of samples with a high level of lncRNA SOX2OT, while in the presence of samples containing small amounts of target are strongly aggregated.

Moreover, the performance of this method was evaluated directly on extracted RNA from ADC and SCC lung cancer samples. As shown in Figure 4A, the difference in LSPR peak was recorded in the presence of SCC with a high level of the target lncRNA SOX2OT (C_t no. < 44) and ADC with a very low expression of RNA (C_t no. > 44) samples. The characteristic LSPR peak of AuNPs at 530 nm shifts to longer wavelength at >550 nm in the presence of ADC samples, with a color change from red to purple.

As shown in Figure 4C, the samples were initially tested using qRT-PCR for lncRNA SOX2OT, and the results were plotted against our LSPR signals at 660 nm. The color difference between the ADC and SCC samples is clearly seen (Figure 4B). These results show that a DNA probe with high specificity and selectivity has been able to hybridize to target, lncRNA SOX2OT, in such a complex solution.

In Table 1, we compared the performance of this colorimetric method with the previously reported methods for detection of long noncoding RNAs.[22−30,30]

3.4. The Specificity and Sensitivity of the Expression Levels of lncRNA SOX2OT in Discriminating AC and SCC Lung Tumor Samples. The qPCR ROC curve analysis (Figure 4D) was employed to investigate the potential suitability of the expression levels of the *lncRNA SOX2OT* spliced transcript to discriminate between ADC and SCC lung cancer samples. Our ROC curve data with an area under the curve (AUC) of 0.836 demonstrated that *lncRNA SOX2OT* can be a suitable biomarker to classify two lung tumor types with high sensitivity and specificity.

4. CONCLUSION

The present study is based on a user-friendly method to detect and distinguish SCC from ADC samples. The biggest challenge with this method is the design of specific probes. After that, two selected probes were designed with an additional G12 tail to act as a scaffold for the in situ synthesis of AuNPs. After the formation of P1@AuNPs and P2@AuNPs, they were used for visible colorimetric sensing of long noncoding RNA SOX2OT due to the different LSPR bands without the requirement of any amplification (RT-PCR) process. The applicability of this approach can be generalized to other lncRNAs only by redesigning two specific probes to selectively target various diseases.

AUTHOR INFORMATION

Corresponding Authors

Seyed Javad Mowla − *Department of Molecular Genetics Faculty of Biological Sciences, Tarbiat Modares University, Tehran 14115-175, Iran*; Email: sjmowla@modares.ac.ir

Yasaman-Sadat Borghei − *Center for Bioscience & Technology, Institute for Convergence Science & Technology Sharif University of Technology, Tehran 1458889694, Iran*; orcid.org/0009-0003-9530-4815; Email: yasaman.borghei@sharif.edu

Authors

Nastaran Roknabadi − *Department of Molecular Genetics Faculty of Biological Sciences, Tarbiat Modares University, Tehran 14115-175, Iran*

Seyedeh Saina Seifezadeh − *Department of Molecular Genetics Faculty of Biological Sciences, Tarbiat Modares University, Tehran 14115-175, Iran*

Bahram M. Soltani − *Department of Molecular Genetics Faculty of Biological Sciences, Tarbiat Modares University, Tehran 14115-175, Iran*

Complete contact information is available at: https://pubs.acs.org/10.1021/acsomega.4c04565

Author Contributions

N.R. and Y.-S.B. contributed equally as first authors.

Notes

The authors declare no competing financial interest.

ACKNOWLEDGMENTS

The authors gratefully acknowledge the Office of Research Affairs of Sharif University of Technology.

REFERENCES

(1) Barta, J. A.; Powell, C. A.; Wisnivesky, J. P. Global Epidemiology of Lung Cancer. *Ann. Global Health* **2019**, *85* (1), 8.

(2) Nicholson, A. G.; Tsao, M. S.; Beasley, M. B.; Borczuk, A. C.; Brambilla, E.; Cooper, W. A.; et al. The 2021 WHO classification of lung tumors: impact of advances since 2015. *Journal of Thoracic Oncology* **2022**, *17* (3), 362−87.

(3) Thakur, S. K.; Singh, D. P.; Choudhary, J. Lung cancer identification: a review on detection and classification. *Cancer metastasis reviews* **2020**, *39* (3), 989−98.

(4) Rekhtman, N.; Ang, D. C.; Sima, C. S.; Travis, W. D.; Moreira, A. L. Immunohistochemical algorithm for differentiation of lung adenocarcinoma and squamous cell carcinoma based on large series of whole-tissue sections with validation in small specimens. *Modern Pathology* **2011**, *24* (10), 1348−59.

(5) Wadowska, K.; Bil-Lula, I.; Trembecki, Ł.; Śliwińska-Mossoń, M. Genetic markers in lung cancer diagnosis: A review. *International journal of molecular sciences* **2020**, *21* (13), 4569.

(6) Yang, J.s.; Li, B.j.; Lu, H.w.; Chen, Y.; Lu, C.; Zhu, R.x.; et al. Serum miR-152, miR-148a, miR-148b, and miR-21 as novel biomarkers in non-small cell lung cancer screening. *Tumor Biology* **2015**, *36* (4), 3035−42.

(7) Nooreldeen, R.; Bach, H. Current and future development in lung cancer diagnosis. *International journal of molecular sciences* **2021**, *22* (16), 8661.

(8) Borghei, Y. S.; Hosseini, M. A New eye Dual-readout Method for MiRNA Detection based on Dissolution of Gold nanoparticles via LspR by Cdte QDs photoinduction. *Sci. Rep.* **2019**, *9* (1), 5453.

(9) Amaral, P. P.; Neyt, C.; Wilkins, S. J.; Askarian-Amiri, M. E.; Sunkin, S. M.; Perkins, A. C.; et al. Complex architecture and regulated expression of the Sox2ot locus during vertebrate development. *RNA (New York, NY)* **2009**, *15* (11), 2013−27.

(10) Wang, Y.; Wu, N.; Luo, X.; Zhang, X.; Liao, Q.; Wang, J. SOX2OT, a novel tumor-related long non-coding RNA. *Biomedicine & Pharmacotherapy* **2020**, *123*, 109725.
(11) Xie, X.; Wang, X.; Liang, Y.; Yang, J.; Wu, Y.; Li, L.; et al. Evaluating Cancer-Related Biomarkers Based on Pathological Images: A Systematic Review. *Frontiers in oncology* **2021**, *11*, 763527.
(12) Cho, W. C.; Zhou, F.; Li, J.; Hua, L.; Liu, F. Biomarker Detection Algorithms and Tools for Medical Imaging or Omics Data. *Front. Genet.* **2022**, *13*, 919390.
(13) Srinivas, P. R.; Barker, P.; Srivastava, S. Nanotechnology in early detection of cancer. *Laboratory investigation* **2002**, *82* (5), 657−62.
(14) Borghei, Y. S.; Hosseini, M.; Ganjali, M. R.; Hosseinkhani, S. A novel dual-mode and label-free aptasensor based methodology for breast cancer tissue marker targeting. *Sens. Actuators, B* **2020**, *315*, 128084.
(15) Borghei, Y. S.; Hosseinkhani, S.; Ganjali, M. R. Plasmonic Nanomaterials": An emerging avenue in biomedical and biomedical engineering opportunities. *Journal of Advanced Research* **2022**, *39*, 61−71.
(16) Borghei, Y. S.; Hosseinkhani, S. Aptamer-based colorimetric determination of early-stage apoptotic cells via the release of cytochrome c from mitochondria and by exploiting silver/platinum alloy nanoclusters as a peroxidase mimic. *Microchim. Acta* **2019**, *186*, 845.
(17) Moros, M.; Kyriazi, M. E.; El-Sagheer, A. H.; Brown, T.; Tortiglione, C.; Kanaras, A. G. DNA-coated gold nanoparticles for the detection of mRNA in live Hydra vulgaris animals. *ACS Appl. Mater. Interfaces* **2019**, *11* (15), 13905−11.
(18) Borghei, Y. S.; Hosseinkhani, S. Building Polyvalent DNA-Functionalized Anisotropic AuNPs using Poly-Guanine-Mediated In-Situ Synthesis for LSPR-Based Assays: Case Study on OncomiR-155. *Photochem. Photobiol.* **2022**, *98* (5), 1043−9.
(19) Saghaeian Jazi, M.; Samaei, N. M.; Mowla, S. J.; Arefnezhad, B.; Kouhsar, M. SOX2OT knockdown derived changes in mitotic regulatory gene network of cancer cells. *Cancer Cell Int.* **2018**, *18* (1), 129.
(20) Kamel, L. M.; Atef, D. M.; Mackawy, A. M.; Shalaby, S. M.; Abdelraheim, N. Circulating long non-coding RNA GAS5 and SOX2OT as potential biomarkers for diagnosis and prognosis of non-small cell lung cancer. *Biotechnology and Applied Biochemistry* **2019**, *66* (4), 634−42.
(21) Saghaeian Jazi, M.; Samaei, N. M.; Ghanei, M.; Shadmehr, M. B.; Mowla, S. J. Overexpression of the non-coding SOX2OT variants 4 and 7 in lung tumors suggests an oncogenic role in lung cancer. *Tumor Biology* **2016**, *37*, 10329−38.
(22) Zhang, Q.; Su, C.; Tian, X.; Zhang, C. Y. Corn-Based Fluorescent Light-Up Biosensors with Improved Signal-to-Background Ratio for Label-Free Detection of Long Noncoding RNAs. *Anal. Chem.* **2023**, *95*, 8097−8104.
(23) Zhang, Y.; Du, X. K.; Liu, W. J.; Liu, M.; Zhang, C. Y. Programmable ligation-transcription circuit-driven cascade amplification machinery for multiple long noncoding RNAs detection in lung tissues. *Anal. Chem.* **2022**, *94*, 10573−10578.
(24) Zhao, N. N.; Yu, X. D.; Tian, X.; Xu, Q.; Zhang, C. Y. Mix-and-detection assay with multiple cyclic enzymatic repairing amplification for rapid and ultrasensitive detection of long noncoding RNAs in breast tissues. *Anal. Chem.* **2023**, *95*, 3082−3088.
(25) Jiang, S.; Liu, T.; Liu, Q.; Zhang, Q.; Han, Y.; Tian, X.; Zhang, C. Y. Rapid, Sensitive, and Label-Free Detection of Long Noncoding RNAs in Breast Cancer Tissues by RecJf Exonuclease-Assisted Recombinase Polymerase Amplification. *Anal. Chem.* **2023**, *95*, 15133−15139.
(26) Zhang, Y.; Wang, C.; Zou, X.; Tian, X.; Hu, J.; Zhang, C. Y. Simultaneous enzyme-free detection of multiple long noncoding RNAs in cancer cells at single-molecule/particle level. *Nano Lett.* **2021**, *21*, 4193−4201.
(27) Shandilya, R.; Kumari, R.; Singh, R. D.; Chouksey, A.; Bhargava, A.; Goryacheva, I. Y.; Mishra, P. K. Gold based nano-photonic approach for point-of-care detection of circulating long non-coding RNAs. *Nanomedicine: Nanotechnology, Biology and Medicine* **2021**, *36*, 102413.
(28) Liu, F.; Xiang, G.; Jiang, D.; Zhang, L.; Chen, X.; Liu, L.; Luo, F.; Li, Y.; Liu, C.; Pu, X. Ultrasensitive strategy based on PtPd nanodendrite/nano-flower-like@ GO signal amplification for the detection of long non-coding RNA. *Biosens. Bioelectron.* **2015**, *74*, 214−221.
(29) Liu, F.; Xiang, G.; Zhang, L.; Jiang, D.; Liu, L.; Li, Y.; Liu, C.; Pu, X. A novel label free long non-coding RNA electrochemical biosensor based on green l-cysteine electrodeposition and Au−Rh hollow nanospheres as tags. *RSC Adv.* **2015**, *5*, 51990−51999.
(30) Islam, M. N.; Moriam, S.; Umer, M.; Phan, H. P.; Salomon, C.; Kline, R.; Nguyen, N. T.; Shiddiky, M. J. Naked-eye and electrochemical detection of isothermally amplified HOTAIR long non-coding RNA. *Analyst* **2018**, *143*, 3021−3028.
(31) Chen, M.; Wu, D.; Tu, S.; Yang, C.; Chen, D.; Xu, Y. A novel biosensor for the ultrasensitive detection of the lncRNA biomarker MALAT1 in non-small cell lung cancer. *Sci. Rep.* **2021**, *11* (1), 3666.
(32) Li, Y.; Liu, L. E.; Han, H.; Yuan, X.; Ji, J.; Xue, L.; Wu, Y.; Yang, R. A signal-switchable photoelectrochemical biosensor for ultrasensitive detection of long non-coding RNA in cancer cells. *Talanta* **2024**, *273*, 125878.
(33) Broto, M.; Kaminski, M. M.; Adrianus, C.; Kim, N.; Greensmith, R.; Dissanayake-Perera, S.; Schubert, A. J.; Tan, X.; Kim, H.; Dighe, A. S.; Collins, J. J.; et al. Nanozyme-catalysed CRISPR assay for preamplification-free detection of non-coding RNAs. *Nat. Nanotechnol.* **2022**, *17* (10), 1120−1126.

https://doi.org/10.1021/acsomega.4c04565
ACS Omega 2024, 9, 37205−37212